

# Articles

## Origin of the Color of $\pi$ -Conjugated Polymers: Poly(*N*-*n*-octyl-3-carbazoyl)acetylene Prepared with a [Rh(norbornadiene)Cl]<sub>2</sub> Catalyst

Masayoshi Tabata,\* Takashi Fukushima, and Yoshikazu Sadahiro

Department of Molecular Chemistry, Graduated School of Engineering, Hokkaido University,  
Sapporo 060-8628, Japan

Received March 19, 2004

**ABSTRACT:** Stereoregular polymerization of (*N*-*n*-octyl-3-carbazoyl)acetylene was successfully performed with a [Rh(NBD)Cl]<sub>2</sub> (NBD = norbornadiene) catalyst to afford poly(*N*-*n*-octyl-3-carbazoyl)acetylene (PNOCzA) as a new type of possible electron-transporting polymer in fairly high yields when triethylamine, chloroform, or dimethylformamide was used as the polymerization solvent. The resulting polymers were composed of amorphous *cis*–*transoid* isomers bearing a yellow color or crystalline *cis*–*transoid* isomers having an orange color, called a columnar, as a  $\pi$ -conjugated molecular assembly at the solid state. The *cis*-to-*trans* isomerization of the yellow and orange polymers was induced by compression at 200 kg/cm<sup>2</sup> under vacuum at room temperature for 10 min. The polymers obtained before and after compression were characterized in detail using <sup>1</sup>H NMR, wide-angle X-ray diffraction, laser Raman, electron spin resonance, and diffuse reflective UV–vis (DRUV–vis) methods. The data showed that compression of the orange polymers resulted in not only destruction of the columnar structure but also formation of a *trans*–*transoid* isomer. The *trans*–*transoid* isomers obtained by compression of the yellow and orange polymers showed to have fairly long *trans* conjugated sequences in which  $\pi$  radicals obtained by the rotational scission of the *cis* C=C bonds can be stabilized as less mobile unpaired electrons. The *trans* conjugation lengths, *n*, in the (C=C)<sub>*n*</sub> created by the compression of the yellow polymer were estimated as ca. 33 and ca. 36 using the DRUV–vis and Raman methods, respectively. The orange polymers bearing the columnar structure were found to show an extremely wide range absorption in the range from 210 nm to a near-infrared region, ~850 nm, compared with that of the yellow polymer, although the compression induced such a *cis*–*trans* isomerization. Therefore, the columnar as the molecular assembly is newly proposed as an important color element in order to control the color of the such conjugated polymer at the solid phase. In the solution <sup>1</sup>H NMR spectrum of the orange polymer observed after the compression, the first methylene proton peak in the *n*-octyl group attached to the nitrogen of the carbazoyl ring was found to be almost smeared out. This phenomenon was explained by magnetic dipole–dipole interaction between the methylene proton and the unpaired electron which migrated from the main chain to the carbazoyl nitrogen moiety through the delocalization of the unpaired electrons which were generated by the rotational scission of the *cis* C=C double bonds in the main chain when compressed.

### Introduction

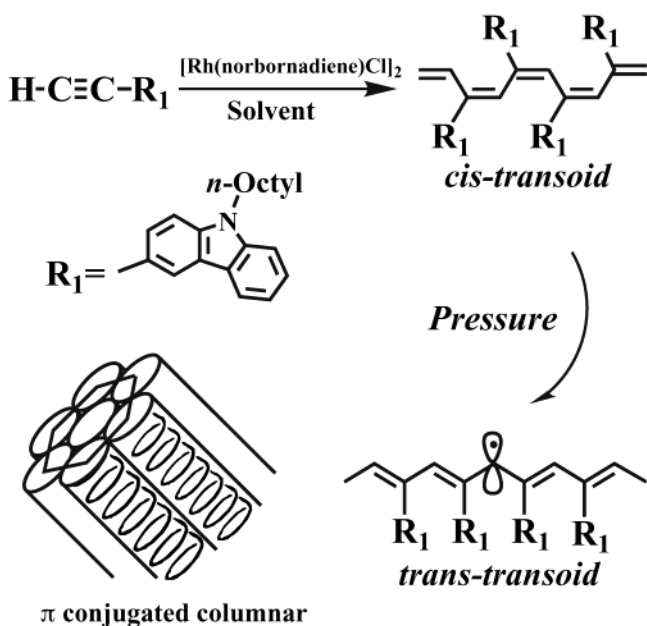
Numerous conjugated polymers have been used as emissive layers in light-emitting diodes (LEDs).<sup>1</sup> Over the past few years, important improvements have been made concerning the control of color, luminescence efficiency, and the durability of polymer LEDs.<sup>2</sup> In particular, blends of conjugated polymers with poly(*N*-vinylcarbazole), PVC, as a hole-transporting matrix have been achieved and have shown significant increase of luminescence efficiency.<sup>3</sup> In this report we show the first stereoregular polymerization of (*N*-*n*-octyl-3-carbazoyl)acetylene, NOCzA, initiated with a [Rh(NBD)-Cl]<sub>2</sub> (NBD = norbornadiene) catalyst in the presence of various solvents such as chloroform, triethylamine (TEA), and dimethylformamide (DMF) at around room temperature to selectively produce the *cis*-poly(carbazoyl)acetylene, PNOCzA, as a new type of possible electron-transporting matrix in very high yields together with detailed characterization of the resulting polymers

using <sup>1</sup>H NMR, laser Raman, diffuse reflective UV–vis (DRUV–vis), electron spin resonance (ESR), and wide-angle X-ray diffraction (XRD) methods.

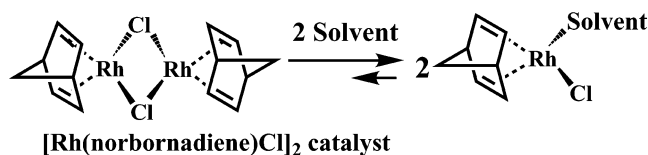
Previously, we reported<sup>4–7</sup> that aromatic acetylenes can be stereoregularly polymerized with the Rh complex catalyst having norbornadiene as the most effective ligand to give the highest yield. Further, we showed that alcohol,<sup>4</sup> amine,<sup>5,6</sup> water,<sup>7</sup> and DMF<sup>7</sup> are quite useful solvents to provide a monomeric Rh complex which may work as the active initiation species as in this stereoregular polymerization.<sup>4–7</sup>

On the other hand, the Ziegler–Natta catalyst, e.g., Et<sub>3</sub>Al–Ti(*On*-Bu)<sub>4</sub>,<sup>8</sup> or metathesis catalyst, e.g., WCl<sub>6</sub> or MoCl<sub>5</sub>,<sup>9</sup> as the so-called Lewis catalysts may be deactivated through hydrolysis or coordination due to their solvents. In this report we also show that a new monomer, i.e., (*N*-*n*-octyl-3-carbazoyl)acetylene, NOCzA, can be polymerized by the Rh complex catalyst to produce the PNOCzA in very high yields even if the

Scheme 1



Scheme 2



carbazoyl group is involved as a strong basic moiety in the monomer. Further, we newly report that the color of the obtained polymer at the solid state is not controlled by the pristine primary polymer structure like repeated single-double bonds but correlated with a secondary structure, e.g., formation of columnar<sup>10</sup> as a new color element of the solid polymer.

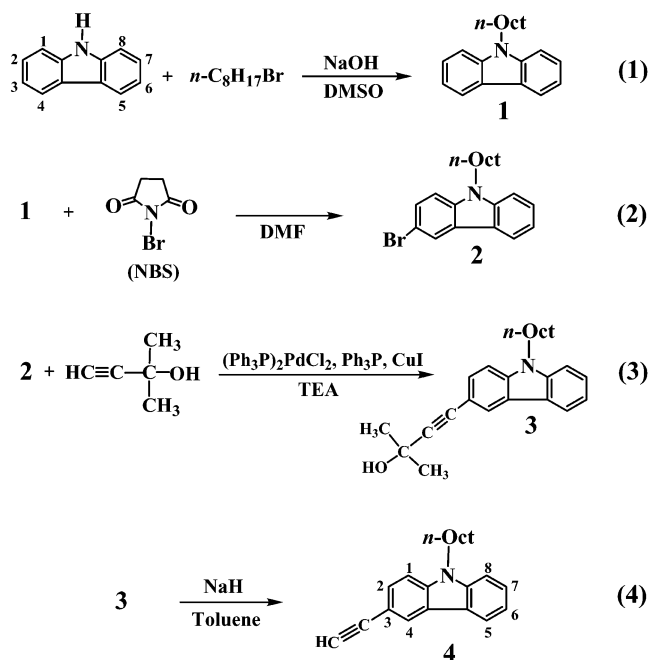
## Experimental Section

**Materials.** All the solvents and products are reagent grade; the monomer, NOCzA, was prepared according to equations shown in Scheme 3.

***N*-*n*-Octylcarbazole, 1.** In a three-necked 250 mL flask equipped with a condenser, dropping funnel, and calcium chloride tube, 25 g (0.15 mol) of carbazole, 43 g (0.22 mol) of *n*-octyl bromide, 2 g (0.009 mol) of triethylammonium chloride, and 120 mL of dimethyl sulfoxide (DMSO) were added and stirred for 1 h under a nitrogen atmosphere, and then 25 mL of an aqueous solution involving 25 g (0.63 mol) of sodium hydroxide was added slowly to the solution. The reaction mixture was stirred for 8 h at ca. 80 °C. Then the reaction mixture was cooled to room temperature and poured into excess water. The resulting crude product was extracted with chloroform. The obtained organic layer was dried with anhydrous magnesium sulfate for 24 h; after that, the solvent was evaporated under reduced pressure to yield a greenish viscous liquid: 40.8 g, yield 97.4%.

**3-Bromo-*N*-*n*-octylcarbazole, 2.** (*N*-*n*-Octyl-3-carbazoyl)-acetylene was prepared as follows: A solution of 25 g (0.15 mol) of carbazole, 43 g (0.22 mol) of *n*-octyl bromide, and 2.0 g (0.009 mol) of triethylammonium chloride in 120 mL of dimethyl sulfoxide, DMSO, was stirred for 1 h under a nitrogen atmosphere, and then 25 mL of an aqueous solution of 25 g (0.63 mol) of sodium hydroxide was added slowly. The mixture was stirred for 8 h for heating. After the reaction, the reaction mixture was cooled to room temperature. The resulting solution was poured into water, and the crude product was extracted with chloroform. The obtained organic layer was

Scheme 3



dried with anhydrous magnesium sulfate for 24 h, and the solvent was evaporated under reduced pressure to yield a greenish viscous liquid: 41 g, yield 97%.

The obtained *N*-*n*-octylcarbazole, **1** (41 g, 0.15 mol), was mixed with 26 g of *N*-bromosuccinimide, NBS, in 300 mL of *N,N*-dimethylformamide, DMF, in the dark and stirred for 3 days at room temperature under a nitrogen atmosphere. After the reaction, the resulting solution was poured into water, and the crude product was extracted with chloroform. The obtained organic layer was dried with anhydrous magnesium sulfate for 24 h, and the solvent was evaporated under reduced pressure. After evaporation, the obtained *N*-*n*-octyl-3-bromocarbazole, **2**, was distilled at 135 °C/10<sup>-3</sup> mmHg to yield a viscous liquid: 11 g, yield 21%.

The *N*-*n*-octyl-3-bromocarbazole, **2** (11 g, 0.030 mol), was mixed with 80 mL of triethylamine, 0.23 g (1.2 mmol) of copper(I) iodide and refluxed, 0.24 g (0.90 mmol) of triphenylphosphine, 0.21 g (0.30 mmol) of dichlorobis(triphenylphosphine)palladium(II), and refluxed for 1 h under a nitrogen atmosphere. 2-Methyl-3-butyn-2-ol was added to the solution and refluxed for 6 h. After the reaction, the resulting solution was poured into water, and the crude product was extracted with chloroform. The obtained organic layer was dried with anhydrous magnesium sulfate for 24 h, and the solvent was evaporated under reduced pressure. After the evaporation, the obtained 3-methyl-1-(*N*-*n*-octylcarbazoyl)-1-butyn-2-ol, **3**, was purified by column chromatography (eluent: chloroform) to yield a viscous liquid: 6.6 g, yield 61%.

The obtained 3-methyl-1-(*N*-*n*-octylcarbazoyl)-1-butyn-2-ol, **3** (6.6 g, 0.018 mol), was mixed with 0.66 g (0.027 mol) of sodium hydroxide and 35 mL of dried toluene and refluxed for 6 h. After the reaction, the resulting solution was poured into water, and the crude product was extracted with chloroform. The obtained organic layer was dried with anhydrous magnesium sulfate for 24 h, and the solvent was evaporated under reduced pressure. After the evaporation, the obtained (*N*-*n*-octyl-3-carbazoyl)acetylene, NOCzA (**4**), was purified by column chromatography (eluent: hexane/toluene, v/v; ratio: 8/1) to yield a viscous liquid: 1.3 g, yield 23%.

**Characterization.** <sup>1</sup>H NMR spectrum was observed on a JEOL JNM-EX 270 MHz using deuterated chloroform, CDCl<sub>3</sub> at room temperature. Polymers were compressed at 100 or 200 kg/cm<sup>2</sup> for 10 min under dynamic vacuum at 10<sup>-2</sup> mmHg at room temperature, using an oil press for manufacturing KBr disk. ESR spectra were recorded on a JEOL FE1XG with 100 kHz field modulation using a temperature control unit. Diffuse

**Table 1.** Polymerization Results of NOCzA with the [Rh(NBD)Cl]<sub>2</sub> Catalyst in the Presence of Various Solvents<sup>a</sup>

run	monomer	solvent	yield (%)	color	$M_n^c$	$M_w/M_n^c$
1	NOCzA	DMF	77.2	yellow	<i>d</i>	<i>d</i>
2	NOCzA	DMF <sup>b</sup>	91.2	yellow	<i>d</i>	<i>d</i>
3	NOCzA	toluene <sup>b</sup>	78.3	orange	<i>d</i>	<i>d</i>
4	NOCzA	THF <sup>b</sup>	80.0	orange	96,000	1.37
5	NOCzA	TEA	98.3	orange	<i>d</i>	<i>d</i>
6	NOCzA	CHCl <sub>3</sub> <sup>b</sup>	94.9	orange	160,000	1.23

<sup>a</sup> Polymerization temperature 30 °C; polymerization time 2 h; [M]/[Cat.] = 150. <sup>b</sup> Polymerized with TEA as a cocatalyst; [Cocat.]/[Cat.] = 100. <sup>c</sup> Measured by GPC using THF as eluent and polystyrene as a standard. <sup>d</sup> Insoluble in chloroform.

reflective UV–vis (DRUV–vis) spectra of the polymer before and after compression were recorded on a JASCO V550 equipped with an ISV-469. Laser Raman spectra were recorded on a JASCO TRS-401 using Ar<sup>+</sup> laser light at 514.5 nm. Gel permeation chromatography (GPC) of the polymer was determined with a JASCO GPC 900-1 instrument with a UV–vis detector using Shodex K-803L and K-806L columns, THF as an eluent, and polystyrene as a standard. Wide-angle X-ray diffraction (XRD) patterns were recorded on a JEOL JDX-3500 with a bent optical crystal monochromator.

**Polymerization.** Poly(*N*-*n*-octyl-3-carbazoyl)acetylene (PNO-CzA) was obtained by treatment of NOCzA, **4**, with the Rh catalyst using different solvents under the same reaction conditions.<sup>4,6–7,11</sup> In a typical procedure, 0.23 g ( $7.6 \times 10^{-4}$  mol) of the monomer and the calculated amount of catalyst were placed in the two tubes of a specially designed U-shaped glass ampule in our laboratory,<sup>10</sup> and the polymerization solvent was introduced into both sides. After the ampule was warmed to 30 °C, the reaction mixture was stirred according to time, as reported in Table 1 at ca.  $10^{-2}$  Torr. The reaction was stopped using an excess amount of methanol, and the resulting polymer was filtered off, washed with methanol, and dried under dynamic vacuum for 24 h. Yields are reported in Table 1. Elemental analysis of run 5 in Table 1 as a typical polymer: Calcd (%) for C<sub>21</sub>H<sub>25</sub>N<sub>1</sub> (MW = 303.44): C, 87.08; H, 8.30; N, 4.62. Found: C, 86.92; H, 8.37; N, 4.60.

## Results and Discussion

**Polymerization.** The monomer NOCzA, was polymerized using the Rh complex, [Rh(NBD)Cl]<sub>2</sub>, catalyst in order to determine the best polymerization conditions. In our previous papers<sup>6,7a</sup> we showed that chloroform and toluene do not work as the cocatalyst for activation of the dimeric Rh catalyst (see Scheme 2). Therefore, TEA was added to the solvent such as DMF or tetrahydrofuran (THF) to make the active species from the Rh complex. The polymerization results are shown in Table 1. The polymerization of runs 1, 2, 3, 5, and 6 did proceed inhomogeneously, but runs 4 and 6 proceeded homogeneously, though each case afforded orange polymers. It is clear that fairly high yields were obtained within 2 h even at 30 °C when a mixed solvent such THF/TEA = 100/1 (v/v) or chloroform/TEA = 100/1 (v/v) was used to produce the soluble polymers with high yields: 80.0–98.3%. The obtained molecular weight and its dispersities were estimated as ca.  $(9.6–16.0) \times 10^4$  and  $M_w/M_n \approx 1.23–1.37$ , respectively. Those polymers (runs 4 and 6 in Table 1) were soluble in chloroform and THF and insoluble in methanol and *n*-hexane. It should be noted that the NOCzA monomer can be newly polymerized when the Rh complex catalyst, even the carbazole moiety as a strong organic base, is included in such solvents, indicating that the basic moiety does not work as the inhibitor or deactivator to the Rh catalyst (see Scheme 2).

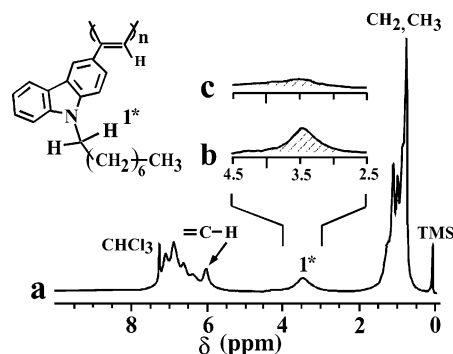


**Figure 1.** <sup>1</sup>H NMR spectra of the PNOcZA polymers (run 6 in Table 1) prepared with [Rh(NBD)Cl]<sub>2</sub> in the presence of TEA: (a) a full-scale spectrum of PNOcZA, (b) an expanded peak of >N–CH<sub>2</sub> protons before compression, and (c) an expanded peak of >N–CH<sub>2</sub> protons after compression at 200 kg/cm<sup>2</sup> under vacuum at room temperature.

**<sup>1</sup>H NMR.** Figure 1a shows the <sup>1</sup>H NMR spectrum of PNOcZA, with an orange color (run 6 in Table 1) observed in CDCl<sub>3</sub> solvent at 30 °C. The peaks observed as a multiplet (15H) at 0.7–1.7 ppm were assigned to those of protons due to the CH<sub>3</sub> and CH<sub>2</sub> groups in the alkyl side chain.<sup>11</sup> The two singlets at 3.49 ppm (2H) and 6.1 ppm (1H) were ascribed to those of the –CH<sub>2</sub> protons at the N atom of the alkyl side chain attached to the carbazole group and =C–H proton in the main chain, respectively.<sup>7</sup> The cis ratio was estimated as ca. 100% because the integrated intensities between the =C–H, N–CH<sub>2</sub>, and the peak area of the alkyl protons from 0.7–1.7 ppm were rigorously estimated as 1:2:15, respectively.<sup>7</sup> This strongly indicates the stereoregular polymerization of the NOCzA monomer, **4**, i.e., no irregular sequences such as head-to-head and/or tail-to-tail structure,<sup>4–7</sup> or a cyclohexadienyl moiety<sup>12,13</sup> as a result of intramolecular cyclization was involved so that such an extremely sharp line width spectrum was observed even despite the high molecular weight,  $M_n = 160,000$  with a cis–transoid form as reported by us.<sup>6–7</sup>

**Compression of Amorphous Polymer.** An orange polymer (see run 6 in Table 1) was compressed under reduced pressure, ca.  $10^{-2}$  Torr for 10 min at room temperature, to determine whether cis-to-trans isomerization is induced as previously reported by us.<sup>6,7</sup> Figure 1c shows the expanded <sup>1</sup>H NMR spectrum of the chemical shifts region in the range of >N–CH<sub>2</sub> protons which were observed in CDCl<sub>3</sub> solvent after compression of the orange polymer. It is clear that the peak shape was extremely broadened, i.e., almost smeared out after the compression despite the solution state. Such line broadening phenomenon has not been reported, to the best of our knowledge, although the so-called cis-to-trans isomerization is induced by the compression to produce planar  $\pi$ -conjugated trans sequences.<sup>14–19</sup> The phenomenon may be related with unpaired electrons which were generated as the  $\pi$  radicals called solitons<sup>20,21</sup> through the rotational scission of the cis C=C bonds, as discussed in detail below.

The ratio of the cis sequences after the compression could be rigorously estimated as ca. 52% from Figure 1a,b comparing the areas of the alkyl proton peaks except for >N–CH<sub>2</sub> with that of the =C–H proton peak observed before and after compression<sup>7a,14a–18</sup> (see Table 2).

The <sup>1</sup>H NMR spectra shown in Figure 1b and c also suggest that the resulting trans polymer is not isomerized to the original cis isomer even when the

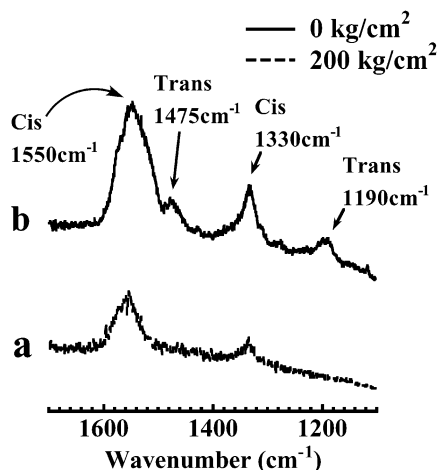


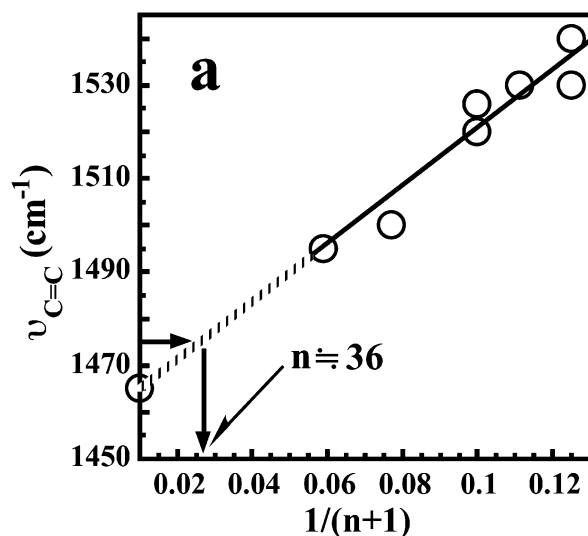
**Figure 2.** Laser Raman spectra of PNOcZA (run 6 in Table 1) observed at room temperature: (a) before compression and (b) after compression at 200 kg/cm<sup>2</sup> under vacuum at room temperature.

**Table 2. Cis Ratio of the PNOcZA Polymer Estimated before and after Compression Using <sup>1</sup>H NMR Spectral Data**

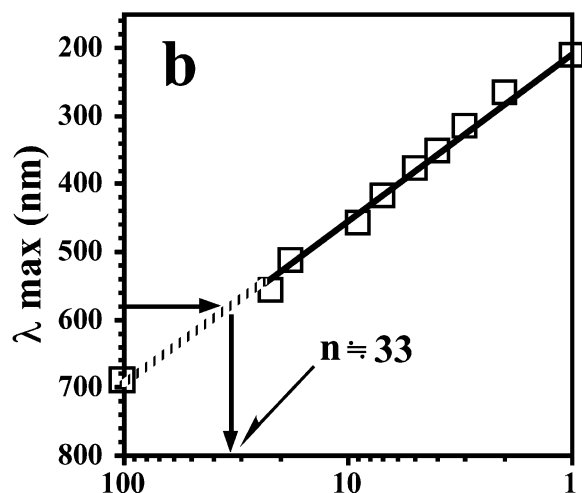
polymer	press. (kg/cm <sup>2</sup> )	proton peak area ratio: CH <sub>3</sub> and (CH <sub>2</sub> ) <sub>6</sub> /=C-H	cis ratio
PNOcZA	0	15/1	100
PNOcZA	200	15/~0.78	52

obtained trans polymer was dissolved in the CDCl<sub>3</sub> solution at room temperature. This isomerization phenomenon will be also proven by the Raman and ESR data observed after the compression as mentioned below.

**Laser Raman. Compression.** Laser Raman spectra were observed to determine what spectral changes are induced by the cis-to-trans isomerization, i.e., when the orange polymer (run 6 in Table 1) was compressed at 200 kg/cm<sup>2</sup> for 10 min under dynamic vacuum at room temperature (see Figure 2a,b) using Ar<sup>+</sup> ion laser light at 514.5 nm. It is clear that, after compression, two peaks at 1190 and 1475 cm<sup>-1</sup> appeared, and the peak intensity at 960 cm<sup>-1</sup> is decreased by the compression, though the peak at 960 cm<sup>-1</sup> is not shown in Figure 2. The two peaks at 1475 and 1190 cm<sup>-1</sup> were assigned to those of the C=C bond and C-C bond vibrations in the resulting trans form, respectively.<sup>14-18,23,24</sup> The peak at 1330 cm<sup>-1</sup> was assigned to that of the C-C bond in the cis form which may be also superposed with that of the bond connecting the main chain with the side chain.<sup>7,11,18,19,22-25</sup> The conjugation length ( $n$ ) was estimated to be  $n = 36$  for 1475 cm<sup>-1</sup>, assuming that the Raman peak of trans polyenes is correlated with the number  $n$  of the trans conjugation length, (C=C) <sub>$n$</sub> ,<sup>25</sup> as shown in Figure 3a. In principle, the resonance Raman (RR) method can only detect the trans conjugation length which can be excited by the wavelength of the laser light used in this experiment, Ar<sup>+</sup> laser light, i.e., 514.5 nm (green color). In other words, more shorter or more longer trans conjugated sequences which are not excited by the Ar<sup>+</sup> laser light cannot be observed even if such trans conjugation lengths are incorporated in the original cis-transoid sequences. Therefore, it should be noted that every kind of trans-transoid sequences cannot be observed, but only some suitable part of trans-transoid sequences which can be excited by the 514.5 nm laser light so that the resonance Raman spectra never show true amount of trans-transoid



**n in trans (C=C)<sub>n</sub> bonds estimated from the Raman spectra.**



**n in trans (C=C)<sub>n</sub> bonds estimated from the diffuse reflective UV spectra.**

**Figure 3.** Dependences of the trans conjugation length, (C=C) <sub>$n$</sub> , on (a) the Raman peak and (b) DRUV-vis peak of PNOcZA (run 5 in Table 1).

sequences but only the trans sequences, selectively,  $n = 36$ , which was generated by the compression. Thus, it was confirmed that compression of other pristine orange and yellow polymers also showed almost the same Raman spectral changes at room temperature in order to create such planar trans  $\pi$ -conjugated sequences as shown in Figure 2b. This strongly indicates that those pristine polymers have also the same cis-transoid form despite the different color, although the differences in the color are discussed using the X-ray data below.

**X-ray Diffraction.** We have shown that conjugated polyacetylenes such as poly(phenylacetylene),<sup>26</sup> poly(*p*-methylphenylacetylene),<sup>27</sup> and poly(alkyl propiolate)<sup>10</sup> called polyacetylene esters, which were stereoregularly prepared with the [Rh(NBD)Cl]<sub>2</sub> catalyst, usually are constituted of a pseudohexagonal structure called a columnar as a  $\pi$ -conjugated self-assembly at the solid state, and the columnar diameter depends on the

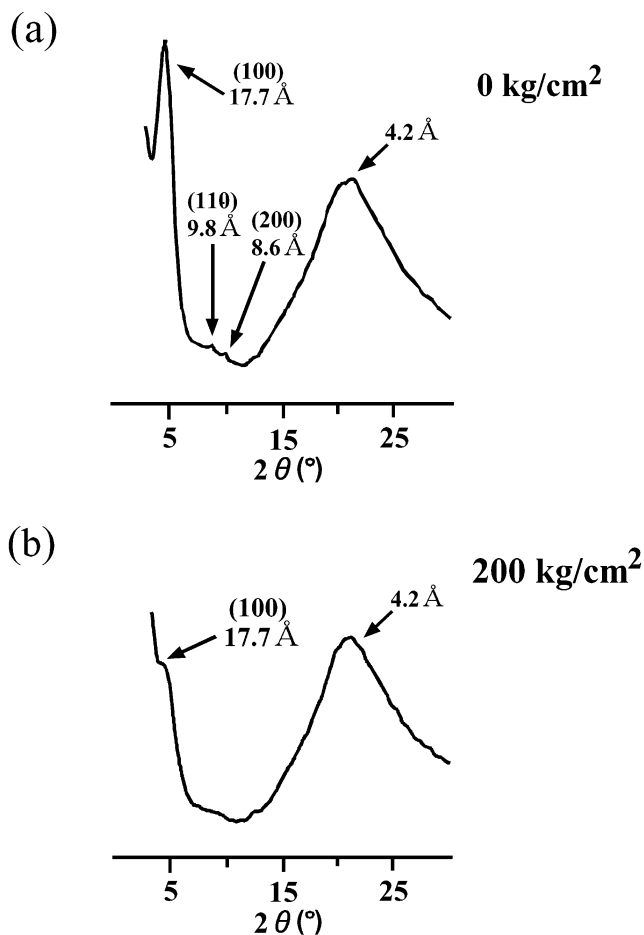


**Figure 4.** XRD of PNOcZA (run 6 in Table 1) (a) before and (b) after compression at 200 kg/cm<sup>2</sup> under vacuum at room temperature.

**Table 3. XRD Parameters of PNOcZA Polymer (Run 6 in Table 1)**

(hkl)	obsd <i>d</i> (Å)	calcd <i>d</i> (Å)	intensity
(100)	17.7	17.7	very strong
(110)	9.8	10.2	very weak
(200)	8.6	8.6	very weak
(400)	4.2	4.4	strong

side chain length of the polymer. We also examined the orange polymer (run 6 in Table 1) to determine whether the pristine polymer is composed of such a columnar using the wide-angle X-ray diffraction (XRD) method (see Figure 4a). The peaks observed at 17.7, ~9.8, ~8.6, and ~4.2 Å were assigned, also assuming formation of the columnar (see Table 3).<sup>10,26–30</sup> Those peaks were attributed to the reflections of (100), (110), (200), and (400), respectively, through a broad peak at around 4.2 Å may be partly superposed with an amorphous halo peak. The crystallinity as the columnar content in this polymer was estimated as ca. 50%. The XRD pattern allowed us to conclude that the pristine polymer is surely consisted of the columnar as the molecular assembly, i.e., the major solid form.

We found, interestingly, that the compression at ca. 200 kg/cm<sup>2</sup> of the orange polymer decreased the intensity of the peak at (100) reflection to a large extent together with a slight decrease of the intensity at ca. 4.2 Å, as shown in Figure 4a,b. This indicates that the columnar content is decreased, i.e., destruction of crystallinity of the columnar by the compression to make the polymer more amorphous. Thus, the columnar

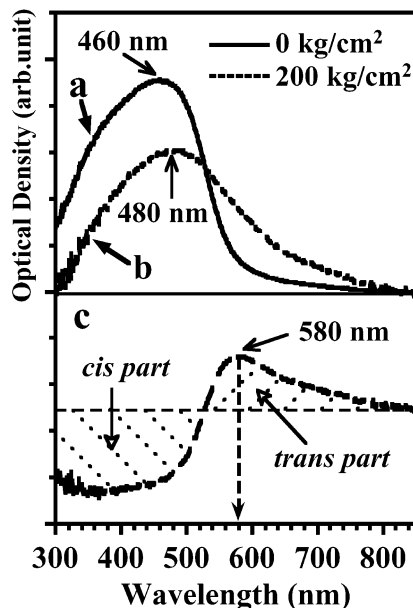


**Figure 5.** Diffuse reflective UV–vis spectra of PNOcZA with a yellow polymer (run 1 in Table 1) observed at room temperature: (a) before and (b) after compression at 200 kg/cm<sup>2</sup> under vacuum at room temperature and (c) the subtraction spectrum.

contents of the pristine orange polymer and compressed polymer were decreased from ca. 50% to ca. 25%.

**Diameter of Columnar.** Previously we have reported<sup>10</sup> that helical main-chain polymers having cis–transoid forms can be stereoregularly prepared with the Rh complex catalyst at around room temperature. It is reasonable to assume, therefore, that the helical main chains are packed in the columns in order to stabilize the columnar structure. Such a columnar is quite unstable if planar polymer chains are packed in each column. The column diameter was estimated as ca. 20.4 Å using the (100) reflection peak observed.

**Diffuse Reflective UV–vis Spectra.** *Compression of Amorphous Polymer.* Figure 5 shows the DRUV–vis spectra observed before and after compression of the yellow polymer (run 1 in Table 1) and the difference spectrum. It is clear that in this experiment compression of the yellow polymer resulted in a large red shift of the absorption maximum from 460 to 480 nm, together with appearance of a new absorption at a longer wavelength region of around 580 nm. The observed large red shift in the yellow polymer may be explained by cis-to-trans isomerization in order to generate new trans  $\pi$ -conjugated sequences.

The length of the resulting trans sequences was also estimated as ca.  $n = 33$ , assuming that the trans conjugation length,  $(C=C)_n$ , is related to the DRUV–vis peak as we have revealed (see Figure 3b).<sup>25</sup> Thus, this trans sequence,  $n = 33$ , generated by the compression, is quite in agreement with that of the trans sequences estimated by the laser Raman data as mentioned above.

**Driving Force of Cis-to-Trans Isomerization:** It should be noted that in the cis–transoid form two aromatic rings are configured in both sides concerning the main chain, and conversely, in the trans–transoid form the large carbazolyl rings are configured in the same direction to the main chain, as shown in Scheme 4. Hence, it may be deduced, reasonably, that the effective molecular volume,  $V(\text{trans})_{\text{eff}}$ , of the trans form is nearly one-half compared with the molecular volume,  $V(\text{cis})_{\text{eff}}$ ,

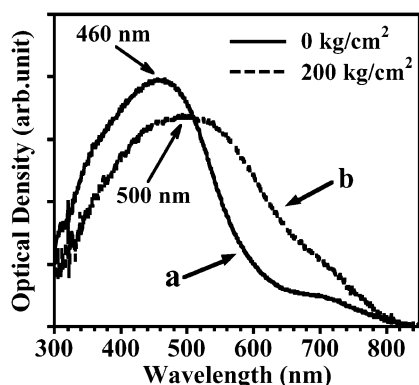
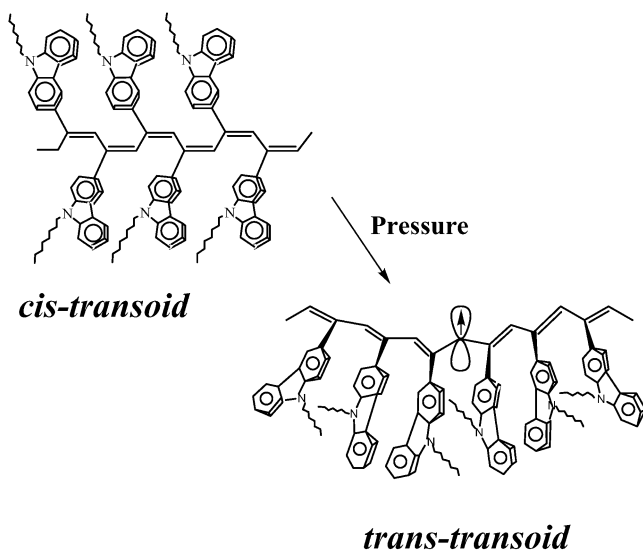


**Figure 6.** Diffuse reflective UV-vis spectra of PNOcZA with orange color (run 6 in Table 1) observed at room temperature: (a) before and (b) after compression at 200 kg/cm<sup>2</sup> under vacuum at room temperature

**Scheme 4**



of the cis-transoid form. Therefore, the compression of the cis form having the more large molecular volume resulted in the decrease of the volume to produce the smaller volume polymer, i.e., trans isomer, inducing the cis-to-trans isomerization as we observed.

$$V(\text{cis})_{\text{eff}}/V(\text{trans})_{\text{eff}} \approx 2\Delta V_{\text{c-t}} \quad (1)$$

**Compression of Columnar Polymer.** Figure 6 shows the DRUV-vis spectra observed before and after compression of the orange polymer (run 6 in Table 1). The pristine orange polymer showed an absorption maximum at 460 nm. It is clear that the pristine orange polymer gives a notably large absorption as an entire peak extending from ca. 300 nm to ca. 820 nm irrespective of the cis-transoid structure as mentioned above. We also found that by the compression the absorption maximum of the orange polymer was shifted to a higher wavelength side, i.e., from  $\lambda_{\text{max}} = 460$  nm to  $\lambda_{\text{max}} \approx 500$  nm together with not only the decrease of absorption intensity in the region from 300 to 505 nm but also the increase in the range of 505–820 nm. Similar absorption spectral changes were observed in other orange polymers before and after the compression. It is suggested, therefore, that the pressure-induced decrease of the absorption intensity in the orange polymer (run 6 in Table 1) is explained in terms of the destruction of the so-called columnar structure at the solid phase. In other

words, the absorption observed in the longer wavelength of the orange polymer may be correlated with the association or aggregation of the columnar polymer chains as  $\pi$ -conjugated molecular assembly or molecular organization as mentioned below.

**Origin of Color.** It should be noted that such a long absorption tail (see Figure 6) observed in the orange columnar polymers has not been observed at the solid phase of the poly(methoxy- and ethoxyphenyl)acetylenes<sup>17,18</sup> which were prepared with the Rh complex catalyst in the presence of ethanol or TEA solvent. Therefore, the new absorption band bearing such an extremely long tail cannot be explained in terms of a classical chromophore, i.e., simple repeated cis-transoid sequences, but rather the formation of a pseudo-hexagonal structure called the  $\pi$ -conjugated columnar as the molecular assembly at the solid state. This orange polymer is also composed of not the trans-transoid form but the cis-transoid form having regular head-to-tail structure as evidenced by not only the Raman at the solid state but also <sup>1</sup>H NMR data in the solution. In other words, this strongly indicates that the spectrum of the orange columnar polymer is attributed to that of specific  $\pi$ -conjugated self-assembly or self-organization. It should be also noted, here, that such simple cis-transoid structures, which are composed of one or two monomer sequences, cannot allow us to explain why the  $\lambda_{\text{max}}$  must be observed at such a longer wavelength region, i.e., at 500 nm. It is suggested, therefore, that such  $\pi$ -conjugated self-assembly or self-organization composed of a pseudo-hexagonal structure called columnar may work as a new effective color controller, i.e., a new color element which can shift the absorption of the cis-transoid polymer to an extremely longer wavelength region despite the cis-transoid form.<sup>33</sup>

**ESR Spectra.** Previously, we have shown<sup>12-18</sup> that the *g* value of not only aromatic but also aliphatic polyacetylenes such as poly(alkyl propiolate)s called polyacetylene esters<sup>10</sup> can be used to deduce the exact geometrical conformation, i.e., cis form or trans form, when one heteroatom such as O, N, or halogen is involved in the side chain of the polyacetylene molecules. Such a heteroatom has a relatively large spin-orbit coupling constant,  $\delta$ ,<sup>31,32</sup> compared with the hydrocarbon radical and the heteroatom can make the observed *g* value shift to lower magnetic field, especially in the cis form. Conversely, such a shift observed in the trans form is extremely small due to decoupling of the magnetic interaction between the side chain and the planar trans main chain.<sup>7,12-18,31</sup> This indicates that the side chain and planar trans conjugation plane are nearly perpendicular to preclude such strong magnetic interaction between the heteroatom in the side chain and the unpaired electrons in the main chain.<sup>7,12-18,31,32</sup> The ESR spectra of the orange polymer (run 6 in Table 1) were also observed to deduce the geometrical structure of the polymers obtained before and after compression under vacuum for 10 min (see Figure 7). The observed parameters are shown in Table 4. It should be noted that compression of the pristine orange polymer (run 6 in Table 1) inversely increased not only the *g* value from 2.0029 to 2.0034 but also the line width,  $\Delta H_{\text{msl}}$ , from 6.0 to 8.0 G, unlike our previous cases,<sup>12-18,31</sup> and the spin concentration was slightly increased from  $6.2 \times 10^{17}$  to  $8.5 \times 10^{17}$  spins/g. We need to explain why such inverse tendencies concerning the *g* value and line width must be observed in this case, although the increase of

**Table 4.** ESR Parameters of PNOCzA Prepared Using Various Solvents in the Presence of  $[\text{Rh}(\text{NBD})\text{Cl}]_2$  Catalyst<sup>a</sup>

polymer	solvent	pressure (kg/cm <sup>2</sup> )	<i>g</i> value		$\Delta H_{\text{msl}}/\text{G}$		spin concn <sup>b</sup> ( $\times 10^{17}$ spins/g)
			RT	77 K	RT	77 K	
PNOCzA	CHCl <sub>3</sub>	0	2.0029	2.0029	6.0	6.2	2.2
		200	2.0034	2.0036	8.0	8.5	2.5
PNOCzA	THF	0	2.0036	2.0028	7.3	12.5	0.4
		200	2.0042	2.0029	8.3	12.2	1.1
PNOCzA	toluene	0	2.0029	2.0032	7.4	10.1	1.1
		200	2.0034	2.0038	7.9	11.9	3.3
PNOCzA	DMF	0	2.0031	2.0027	5.9	6.8	1.5
		200	2.0030	2.0028	7.6	7.9	2.2

<sup>a</sup> Observed at room temperature or 77 K under vacuum. <sup>b</sup> Measured at room temperature.

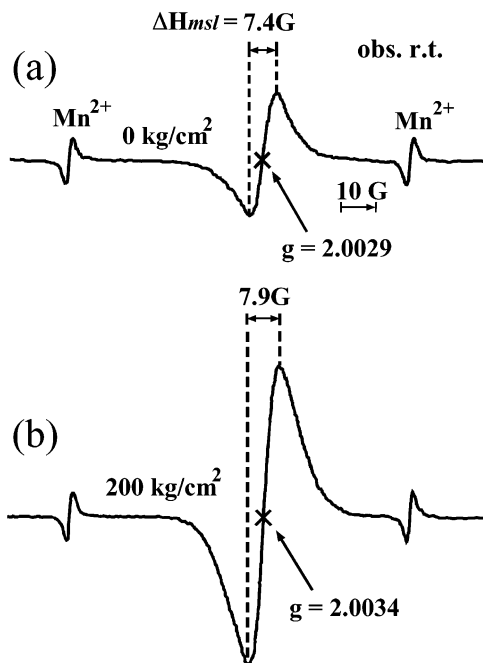
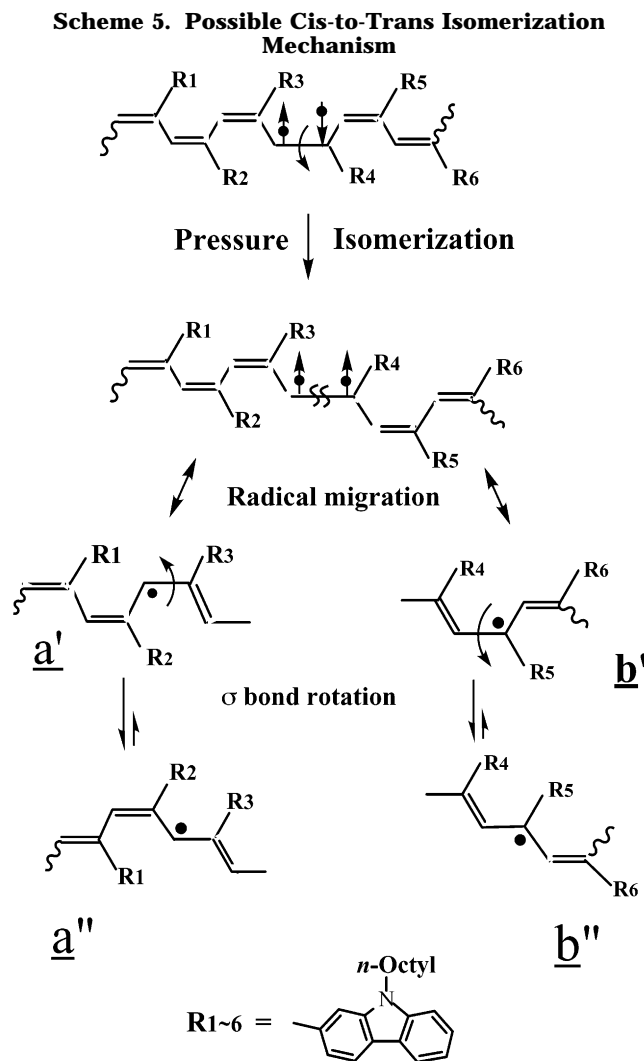


**Figure 7.** ESR spectra of PNOCzA observed at room temperature: (a) before and (b) after compression at 200 kg/cm<sup>2</sup> under vacuum at room temperature. Mn<sup>2+</sup> shown in this figure is used as a standard signal of magnetic field.

the spin concentration strongly supports the compression-induced isomerization from cis form to trans form.<sup>11–18</sup> The compression of the polymer under vacuum can induce the rotational scission of cis C=C bonds to produce two radical spins as biradicals, as mentioned above (see Scheme 5).

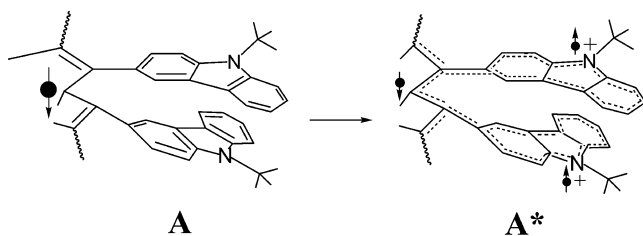
**Radical Migration.** The resulting radical spins may migrate to both sides of the main chains to generate new planar trans sequences as mobile unpaired electron (**a'**) and less mobile unpaired electron (**b'**). However, the motional narrowing effect concerning the line width will be not observed clearly if the resulting trans sequences are not fairly planar but bent structures, unlike our previous cases.<sup>12–18,31</sup> Further, the  $g = 2.0034$  observed after the compression of the orange polymer is fairly large compared with that of the pristine orange polymer. This suggests that in the compressed polymer the unpaired electron produced by the rotational scission of one cis C=C bond delocalize to magnetically interact with a carbazolyl nitrogen bearing the fairly large spin-orbit-coupling constant,  $\delta$ ,<sup>31–33</sup> where two nitrogen cation radicals may be produced because of the electron-donating property in the carbazolyl moiety (see Table 4). Thus, the observed ESR parameters are reasonably explained in terms of the bent trans sequences and the radical migration even after the compression.



Thus, these ESR data support that the pristine orange polymer can be assigned to the cis polymer as proven by not only Raman data but also DRUV-vis without any inconsistency.

Figure 1c showed that in the solution <sup>1</sup>H NMR spectrum observed after the compression of the orange polymer (see run 6 in Table 1) the chemical shift due to the  $\text{N-CH}_2$  peak was almost smeared out. This may be explained by the line-broadening phenomenon, i.e., the so-called dipole-dipole magnetic interaction between the  $-\text{CH}_2$  protons and unpaired electrons which were created by the rotational scission of the cis C=C bonds in the main chain, as shown in Scheme 5. Then two unpaired electrons, **a'** and **b'**, may be created by one double-bond scission, as mentioned above. We examined whether the spin density is partly localized

Scheme 6. Possible Structure of Radical: a



in model structures, **A** or **A\*** (see Scheme 6), using the so-called semiempirical quantum chemical calculation, AM1 method. The calculation indicated that more than one-third of the spin density appeared on the each carbazoyl nitrogen of the main-chain spin density. This structure will be visualized as case **A\***, where the unpaired electron created by rotational scission of the cis C=C bond delocalized even over the carbazoyl moiety, i.e., the nitrogen moiety. In other words, this delocalized structure means that the unpaired electrons migrate to the side chain moiety, i.e., carbazoyl group to meet an electron released by the carbazoyl nitrogen moiety as a strong electron donor group forming the so-called nitrogen radical cation (see **A\*** in Scheme 6).<sup>32</sup> On the other hand, before the compression two cis form radicals, e.g., **a'** and/or **b'**, are created as localized main-chain radicals so that the so-called motional narrowing in the line width is not expected, but a larger  $g$  value may be observed. Thus, we can reasonably explain the reason why the  $g$  value, 2.0034, in the ESR spectra observed after the compression is larger than the  $g = 2.0029$  before the compression. Another main-chain radical, **b'**, was also examined to determine the spin density. However, the radical **b'** structure did not satisfy the observed experimental results, unlike the case **a'**. Thus, the calculated large spin density on the carbazoyl nitrogen clearly explains the reason why the  $\text{N}-\text{CH}_2$  proton peak is broadened after the compression in terms of the so-called magnetic dipole-dipole interaction between the unpaired electrons on the nitrogen and the methylene protons in the chloroform- $d_1$  solution.

This calculation suggests that at least the original direction of the adjacent two alkyl groups in the carbazoyl moieties, **R2** and **R3** (see Schemes 4 and 5), is opposite each other to compensate for the dipole moment of the carbazoyl moiety as such large side groups, although direction of the other carbazoyl group is unclear.

Finally, it should be also noted that the calculated spin densities on the two carbazoyl moieties are nearly equal to each other, and the sign of the magnetic spin in the main-chain carbon is  $\downarrow$ . On the other hand, the signs of the two nitrogens are  $\uparrow$ , as shown in Scheme 6. Therefore, this polymer obtained after the compression may be classified as a promising anti and/or ferromagnetic polymer similar to a model predicted by Ovchinnikov et al.<sup>33</sup>

## Conclusion

Poly(*N*-*n*-octyl-3-carbazoyl)acetylene, p(NOCzA), was stereoregularly prepared using the Rh complex catalyst,  $[\text{Rh}(\text{NBD})\text{Cl}]_2$ , in the presence of various solvents at around room temperature to selectively produce the corresponding cis-transoid polymer in high yields. The poly(NOCzA)s obtained before and after compression were characterized in detail using conventional analytical methods. Consequently, the pristine polymer pre-

pared using various solvents manifested that the yellow or orange color of the polymers is ascribed to formation of the columnar as the  $\pi$ -conjugated self-assembly whose content can be also decreased with compression associated with a large red shift of the absorption maximum in the UV-vis spectrum of the original polymer. Thus, formation and destruction of the columnar as  $\pi$ -conjugated self-assembly is a very important concept for the color design of  $\pi$ -conjugated polymers because an absorption maximum in the conjugated polymer is correlated with not only the color but also the ionization potential. Therefore, the columnar formation at the solid phase becomes a new useful method to control the color of the conjugated polymer even in the cis-transoid form without formation of trans polymers; this color element works as a new concept concerning promising molecular designs for advanced materials such as non-linear optical (NLO)<sup>34-36</sup> or LED<sup>37,38</sup> materials used at the solid state. At present, the origin of color of other aromatic polyacetylenes as well as aliphatic polyacetylenes is being examined more in detail together with the color of the cast film of the polymers. Experiments regarding the pressure-induced cis-to-trans isomerization are in progress in our laboratory, and the results will be published elsewhere soon.

## References and Notes

- Burroughs, J. H.; Bradley, D. D. C.; Brown, A. R.; Marks, R. N.; Mackay, K.; Friends, R. H.; Burn, P. L.; Holmes, A. B. *Nature (London)* **1990**, *347*, 539.
- Cf. e.g. reviews on the chemistry of electroluminescent polymers in: (a) Feast, W. J.; Tsibouklis, J.; Pouwer, K. L.; Groenendale, L.; Meijer, E. W. *Polymer* **1996**, *37*, 5017. (b) Kraft, A.; Grimsdale, A. C.; Holmes, A. B. *Angew. Chem., Int. Ed.* **1998**, *37*, 402. (c) Segura, J. L. *Acta Polym.* **1998**, *49*, 319. (d) Kim, D. Y.; Cho, H. N.; Kim, C. Y. *Prog. Polym. Sci.* **2000**, *25*, 1089.
- Cf. e.g. reviews on molecular OLEDs in: (a) Chen, C. H.; Shi, J.; Tang, W. C. *Macromol. Symp.* **1998**, *125*, 1. (b) Zhang, C.; von Seggern, H.; Pakbaz, K.; Kraabel, B.; Schmidt, H.; Heeger, A. J. *Synth. Met.* **1994**, *62*, 35. (c) Hu, B.; Yang, Z.; Karasz, F. E. *J. Appl. Phys.* **1994**, *76*, 2419.
- (a) Tabata, M.; Yang, W.; Yokota, K. *Polym. J.* **1990**, *22*, 1105. (b) Tabata, M. *Nikkei New Mater.* **1988**, No. 9, 88. (c) Tabata, M.; Yang, W.; Yokota, K. *Polym. Prepr.* **1987**, No. 7, 2090.
- Yang, W.; Tabata, M.; Kobayashi, S.; Yokota, K.; Shimizu, A. *Polym. J.* **1991**, *23*, 1135.
- Tabata, M.; Yang, W.; Yokota, K. *J. Polym. Sci., Polym. Chem. Ed.* **1994**, *32*, 1113.
- (a) Mawatari, Y.; Tabata, M.; Sone, T.; Ito, K.; Sadahiro, Y. *Macromolecules* **2001**, *34*, 3776. (b) Tang, B. Z.; Poon, W. H.; Lueng, S. M.; Leung, W. H.; Peng, H. *Macromolecules* **1997**, *30*, 2209.
- Shirakawa, H.; Ikeda, S. *Polym. J.* **1971**, *2*, 231.
- Masuda, T.; Higashimura, T. *Adv. Polym. Sci.* **1987**, *81*, 121.
- Tabata, M.; Inaba, Y.; Yokota, K.; Nozaki, Y. *J. Macromol. Sci., Pure Appl. Chem.* **1994**, *A31*, 465.
- Tabata, M.; Boucard, V.; Adès, D.; Siove, A.; Sone, T.; Seino, T.; Mawatari, Y. *Macromolecules* **2001**, *34*, 8101.
- Kunzler, J.; Percec, V. *J. Polym. Sci., Polym. Chem. Ed.* **1990**, *28*, 1221 and references therein.
- Dumitrescu, S.; Percec, V.; Simionescu, C. I. *J. Polym. Sci., Polym. Chem. Ed.* **1977**, *15*, 2893.
- (a) Tabata, M.; Sone, T.; Sadahiro, Y. *Macromol. Chem. Phys.* **1999**, *200*, 265. (b) Fujita, Y.; Misumi, Y.; Tabata, M.; Masuda, T. *J. Polym. Sci., Part A: Polym. Chem.* **1998**, *36*, 3157.
- Tabata, M.; Takamura, H.; Yokota, K.; Nozaki, Y.; Hoshina, T.; Minakawa, H.; Kodaira, K. *Macromolecules* **1994**, *27*, 6234.
- Tabata, M.; Tanaka, Y.; Sadahiro, Y.; Sone, T.; Yokota, K.; Miura, I. *Macromolecules* **1997**, *30*, 5200.
- Tabata, M.; Sone, T.; Sadahiro, Y.; Yokota, K.; Nozaki, Y. *J. Polym. Sci., Part A: Polym. Chem.* **1998**, *36*, 217.

- (18) Tabata, M.; Sone, T.; Sadahiro, Y.; Yokota, K. *Macromol. Chem. Phys.* **1998**, *199*, 1161.
- (19) D'Amato, R.; Sone, T.; Tabata, M.; Sadahiro, Y.; Russo, M. V.; Furlani, A. *Macromolecules* **1998**, *31*, 8660.
- (20) Su, W. P.; Schreffer, J. R.; Heeger, A. J. *Phys. Rev. Lett.* **1980**, *44*, 356.
- (21) Mehring, M.; Seidel, H.; Muller, W.; Wegner, G. *Solid State Commun.* **1983**, *45*, 1072.
- (22) Minakawa, H.; Tabata, M.; Yokota, K. *J. Macromol. Sci., Pure Appl. Chem.* **1996**, *A33*, 291.
- (23) Tabata, M.; Namioka, M.; Yokota, K. *Polymer* **1996**, *37*, 1959.
- (24) Tabata, M.; Nozaki, Y.; Yokota, K. *J. Photopolym. Sci. Tech.* **1993**, *6*, 1.
- (25) Harada, T.; Tasumi, M.; Shirakawa, H.; Ikeda, S. *Chem. Lett.* **1978**, 1411.
- (26) Tabata, M.; Kobayashi, S.; Sadahiro, Y.; Nozaki, Y.; Yokota, K.; Yang, W. *J. Macromol. Sci., Pure Appl. Chem.* **1997**, *A34*, 641.
- (27) Tabata, M.; Sadahiro, Y.; Yokota, K.; Kobayashi, S. *Jpn. J. Appl. Phys., Part 1* **1996**, *35*, 5411.
- (28) Kozuka, M.; Sone, T.; Tabata, M.; Enoto, T. *Macromol. Chem. Phys.* **2001**, *201*.
- (29) (a) Tabata, M.; Sadahiro, Y.; Nozaki, Y.; Inaba, Y.; Yokota, K. *Macromolecules* **1996**, *29*, 6673. (b) Tabata, M.; Sadahiro, Y.; Sone, T.; Inaba, Y.; Yokota, K. *Kobunshi Ronbunshu* (in Japanese) **1999**, *56*, 350.
- (30) Unger, G. *Polymer* **1993**, *34*, 2050.
- (31) Pshchetskii, S. Y.; Kotov, A. G.; Milincuk, V. A.; Rozinskii, V. I.; Tupikov, V. I. *ESR of Free Radicals in Radiation Chemistry*; Wiley: New York, 1972; p 22.
- (32) Tabata, M.; Lund, A. *Chem. Phys.* **1983**, *75*, 379.
- (33) Korshak, Y. V.; Medvedeva, T. V.; Ovchinnikov, A. A.; Spector, V. *Nature (London)* **1987**, *32*, 370.
- (34) Neher, D.; Wolf, A.; Bubeck, C.; Wegner, G. *Chem. Phys. Lett.* **1989**, *163*, 116.
- (35) Tabata, M.; Sone, T.; Yokota, K.; Wada, T.; Sasabe, H. *Nonlinear Opt.* **1999**, *22*, 341.
- (36) Wada, T.; Wang, L.; Okawa, H.; Masuda, T.; Tabata, M.; Wan, M.; Kakimoto, M.-A.; Imai, Y.; Sasabe, H. *Mol. Cryst. Liq. Cryst.* **1997**, *294*, 245.
- (37) Bredas, J. L.; Adant, C.; Tacks, P.; Persoons, A.; Pierce, M. *Chem. Rev.* **1994**, *94*, 243.
- (38) Tada, K.; Sawada, H.; Kyokane, J.; Yoshino, K. *Jpn. J. Appl. Phys.* **1995**, *34*, L1083.

MA049454X